

Figure 1 | Supersolid component. The superfluid fraction in crystalline ^4He in the low-temperature limit, as a function of pressure, from Kim and Chan's data^{1,3}. Crystals grown at constant pressure and temperature (2006 data)³ show somewhat less variation in the supersolid fraction than do those grown at constant volume (2004 data)¹. The fraction also does not decrease sharply with increasing pressure, as would be expected if the phenomenon were the result of quantum-mechanical exchange processes in a perfect crystal. The solid line is a guide to the eye.

component should have flowed immediately through the fine pores, but no superflow was observed. This year, however, Sasaki and colleagues⁶ have observed bulk superflow. Again, it is not seen in all samples, but only in those that have a large, observable boundary between two grains (regions of distinct crystallographic orientations) extending across the sample. Superflow seems to occur along, or close to, these grain boundaries.

To understand the significance of these results^{3–6}, one must first know that there are two prevalent pictures of superfluidity. The first of these focuses on the quantum-mechanical exchange, or tunnelling, of atoms between lattice sites. At low temperature, the de Broglie wavelength of ^4He atoms — a quantum-mechanical measure of a particle's extent in space — is long and covers many sites. A long wavelength enables long-range exchange of atoms between lattice sites. If the exchanges extend right across the sample, superfluidity occurs.

The second picture is based on the phenomenon of Bose–Einstein condensation. Any number of the particles known as bosons, which possess integer spin, may occupy a single quantum state. If, at low temperature, a macroscopic fraction of bosons condenses into a single state, a long-range coherence is brought to the system that makes superfluidity possible. In liquid ^4He , the classic superfluid, Bose–Einstein condensation is known to occur below the critical temperature for superfluidity in this system, 2.17 K. As the temperature approaches absolute zero — where ρ_s is 100% — the condensed fraction is around 7%.

Early theoretical discussions^{8–10} of possible superflow in solid ^4He involved quantum tunnelling through ground-state vacancies (these

are lattice sites that are vacant at absolute zero), as well as Bose–Einstein condensation and quantum exchanges within the lattice. The predicted¹⁰ superfluid fraction within the lattice was of the order 0.01%. Unfortunately, however, ground-state vacancies have not been observed in solid ^4He . Thermally activated vacancies are found — but at temperatures above T_C that are irrelevant to the establishment of superfluidity. Recent calculations¹¹ also find that individual vacancies are not stable in the ground state of crystalline ^4He . The vacancies instead coalesce or migrate to a surface; this is the mechanism by which thermal vacancies leave a classical crystal when it is cooled.

Calculations have also shown that there is no long-range coherence, and so no Bose–Einstein condensation, in a perfect crystal of ^4He , essentially because condensation requires double occupancy of a lattice site^{12,13}. In real crystals, the condensate fraction is observed in neutron-scattering experiments¹⁴ to be $0.2 \pm 0.6\%$ — that is, compatible with zero — at a temperature of 0.08 K. Similarly, long-range quantum exchanges within crystalline ^4He are too infrequent to explain the high ρ_s observed¹⁵. As seen in solid ^3He , quantum exchange rates decrease dramatically as a solid is compressed under pressure. If the superfluid fraction arises from exchanges of particles between lattice sites, ρ_s should decrease by orders of magnitude under increasing pressure. But Kim and Chan³ find ρ_s to be largely independent of pressure (Fig. 1). Superflow in crystalline ^4He thus does not seem to be a phenomenon of the perfect bulk solid^{11–13,15}, or to involve individual point defects (vacancies) that are in equilibrium at absolute zero.

Given the recently discovered dependence

of ρ_s on sample annealing^{3–5}, and the correlation of superflow with grain boundaries⁶, supersolidity seems to hinge on macroscopic, long-range defects such as grain boundaries or amorphous channels in the helium crystal. But at the same time, a superfluid density of the same magnitude is observed¹ in helium confined in a nanoporous medium such as Vycor. It is difficult to imagine that extended defects could be the same in helium thus confined and in bulk helium. The situation is far from clear: revealing the secrets of this latest superfluid is very much a work in progress. ■ Henry R. Glyde is in the Department of Physics and Astronomy, University of Delaware, Newark, Delaware 19716, USA.

e-mail: glyde@udel.edu

- Kim, E. & Chan, M. H. W. *Nature* **427**, 225–227 (2004).
- Kim, E. & Chan, M. H. W. *Science* **305**, 1941–1944 (2004).
- Kim, E. & Chan, M. H. W. *Phys. Rev. Lett.* **97**, 115302 (2006).
- Rittner, A. S. C. & Reppy, J. D. *Phys. Rev. Lett.* **97**, 165301 (2006).
- Shirahama, K., Kondo, M., Takada, S. & Shibayama, Y. *Am. Phys. Soc. March Meet. Abstr.* G41.00007 (2006).
- Sasaki, S., Ishiguro, R., Caupin, F., Maris, H. J. & Balibar, S. *Science* **313**, 1098–1100 (2006).
- Day, J. & Beamish, J. *Phys. Rev. Lett.* **95**, 105304 (2006).
- Andreev, A. F. & Lifshitz, I. M. *Sov. Phys. JETP* **29**, 1107–1113 (1969).
- Chester, G. V. *Phys. Rev. A* **2**, 256–258 (1970).
- Leggett, A. J. *Phys. Rev. Lett.* **25**, 1543–1546 (1970).
- Boninsegni, M. *Phys. Rev. Lett.* **97**, 080401 (2006).
- Boninsegni, M., Prokof'ev, N. & Svistunov, B. *Phys. Rev. Lett.* **96**, 105301 (2006).
- Clark, B. K. & Ceperley, D. M. *Phys. Rev. Lett.* **96**, 105302 (2006).
- Diallo, S. O., Pearce, J. V., Taylor, J. W., Kirichek, O. & Glyde, H. R. *Quantum Fluids and Solids Symp. Kyoto, August 2006* (in the press).
- Ceperley, D. M. & Bernu, B. *Phys. Rev. Lett.* **93**, 155303 (2004).

OCEANOGRAPHY

Plankton in a warmer world

Scott C. Doney

Satellite data show that phytoplankton biomass and growth generally decline as the oceans' surface waters warm up. Is this trend, seen over the past decade, a harbinger of the future for marine ecosystems?

Oranges in Florida, wildfires in Indonesia, plankton in the North Pacific — what links these seemingly disparate items is that they are all affected by year-to-year fluctuations in global-scale climate. On page 752 of this issue, Behrenfeld *et al.*¹ describe how such fluctuations, especially in temperature, are connected to the productivity of phytoplankton in the world's oceans. Their analyses are based on nearly a decade of satellite data, and for much of the oceans they find that recent warmer surface temperatures correspond to lower oceanic biomass and productivity. Behrenfeld *et al.* argue that these patterns arise because

climate-induced changes in ocean circulation reduce the supply of nutrients needed for photosynthesis.

Small photosynthetic phytoplankton grow in the well-illuminated upper ocean, forming the base of the marine food web and supporting the fish stocks we harvest. They also form the basis of the biogeochemical cycling of carbon and many other elements in the sea. Phytoplankton growth depends on temperature and the availability of light and nutrients, including nitrogen, phosphorus, silicon and iron. Most of this nutrient supply to the surface ocean comes from the mixing and upwelling of cold, nutrient-rich

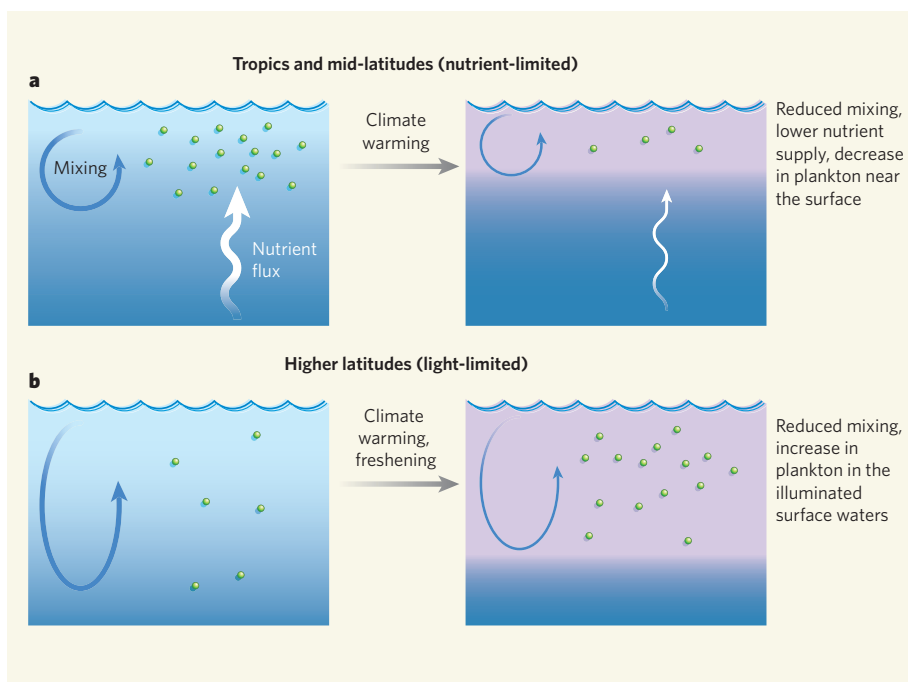


Figure 1 | Predicted phytoplankton response to increased temperature in ocean surface waters¹. **a**, In the tropics and at mid-latitudes, phytoplankton are typically nutrient-limited, and satellite data tie reduced biological productivity to upper-ocean warming and reduced nutrient supply. **b**, At higher latitudes, the opposite biological response to future warming, and extra freshwater input, may occur. In these regions, phytoplankton are often light-limited; reduced mixing would keep plankton close to the surface where light levels are higher.

water from below, with an additional source of iron from mineral dust swept off the continental deserts. Phytoplankton biomass can vary by a factor of 100 in surface waters; its geographical distribution is determined largely by ocean circulation and upwelling, with the highest levels being found along the Equator, in temperate and polar latitudes, and along the western boundaries of continents.

Although the broad spatial patterns of phytoplankton biomass and productivity are well documented², large-scale temporal variations have only recently become quantifiable with the advent of satellite ocean-colour sensors³. The ocean is vast, and the limited number of research ships move at about the speed of a bicycle, too slow to map the ocean routinely on ocean-basin to global scales. By contrast, a satellite can observe the entire globe, at least the cloud-free areas, in a few days. Phytoplankton biomass and growth rates can be estimated remotely from space because chlorophyll, the main photosynthetic pigment in phytoplankton, absorbs blue and red sunlight more readily than green sunlight. Ocean-colour sensors measure, by wavelength band, the small fraction of sunlight scattered back to space from below the surface. The resulting surface-chlorophyll data can be combined with empirical relationships to estimate phytoplankton growth rates or net primary production⁴.

Not that this procedure is straightforward: other constituents of sea water absorb light; many photons reaching the satellite sensor come from atmospheric aerosols or reflection at the water surface; and optical detectors on

satellites degrade with time. But with careful calibration, high-quality, long-term records of ocean-colour data can be constructed for detecting climate-driven trends. The best such record at present is from GeoEye and from NASA's Sea-viewing Wide Field-of-view Sensor (SeaWiFS)³, launched in 1997. In the SeaWiFS time series, global chlorophyll and productivity increase sharply during 1997–98 and then decline gradually to 2005.

Behrenfeld *et al.*¹ show that these trends closely follow changes in climate. The phytoplankton increase in 1997–98 matches a negative (cold) phase of the El Niño–Southern Oscillation (ENSO), and the subsequent slow drop occurred as the planet moved into an extended warm ENSO period. ENSO is a dominant mode of interannual climate variability, and involves large-scale reorganizations of atmosphere and ocean circulation that originate in the equatorial Pacific and extend across the globe. Decreases in productivity are equally well related to increases in sea surface temperatures and vertical temperature gradients in the upper ocean.

The climate–plankton link is found primarily in the tropics and mid-latitudes, where there is limited vertical mixing because the water column is stabilized by thermal stratification (that is, when light, warm waters overlie dense, cold waters). In these areas, the typically low levels of surface nutrients limit phytoplankton growth. Climate warming further inhibits mixing, reducing the upward nutrient supply and lowering productivity (Fig. 1a). At higher latitudes, phytoplankton

are often light-limited because intense vertical mixing carries them hundreds of metres down into darkness where sunlight does not penetrate. In these regions, future warming and a greater influx of fresh water, mostly from increased precipitation and melting sea-ice, will contribute to reduced mixing that may actually increase productivity⁵ (Fig. 1b).

The recent observed global surface warming (about 0.2 °C per decade) is expected to accelerate in coming decades as we continue to release excess carbon dioxide into the atmosphere. In fact, the planet may soon be warmer than at any time in the past million years⁶. Extrapolating the satellite observations into the future suggests that marine biological productivity in the tropics and mid-latitudes will decline substantially, in agreement with climate-model simulations^{7–9}. In those simulations, the geographical boundaries that separate specific marine ecosystems (the ocean equivalents of forests, grasslands and so on) migrate towards the poles, and productivity increases at high latitudes because of surface warming, enhanced freshwater input and reduced deep mixing. Ecosystem dynamics are complex and nonlinear, however, and unexpected phenomena may arise as we push the planet into this unknown climate state. For example, oceanic fixation of atmospheric nitrogen into biologically available forms is concentrated in warm, nutrient-poor surface waters; under more stratified conditions, fixation might increase and enhance overall productivity^{8,10}.

Detecting the impact of climate change requires increased and more sophisticated monitoring of ocean biology and environmental change, both from space and with instruments in the water. Ideally, we need measures not only of such parameters as chlorophyll concentration and productivity, but also of plankton taxonomy (what is there?) and physiology (how healthy are they?). New remote-sensing technologies may help meet these challenges¹¹.

Scott C. Doney is in the Marine Chemistry and Geochemistry Department, Woods Hole Oceanographic Institution, Woods Hole, Massachusetts 02543, USA.
e-mail: sdoney@whoi.edu

- Behrenfeld, M. J. *et al. Nature* **444**, 752–755 (2006).
- Longhurst, A. *Ecological Geography of the Sea* 2nd edn (Academic, New York, 2006).
- McClain, C. R., Feldman, G. C. & Hooker, S. B. *Deep-Sea Res.* **51**, 5–42 (2004).
- Carr, M.-E. *et al. Deep-Sea Res.* **53**, 741–770 (2006).
- Polovina, J. J., Mitchum, G. T. & Evans, G. T. *Deep-Sea Res.* **42**, 1701–1716 (1995).
- Hansen, J. *et al. Proc. Natl Acad. Sci. USA* **103**, 14288–14293 (2006).
- Bopp, L. *et al. Glob. Biogeochem. Cycles* **15**, 81–99 (2001).
- Boyd, P. W. & Doney, S. C. *Geophys. Res. Lett.* **29**, 1806 (2002).
- Sarmiento, J. L. *et al. Glob. Biogeochem. Cycles* **18**, GB3003; doi:10.1029/2003GB002134 (2004).
- Karl, D. *et al. Nature* **388**, 533–538 (1997).
- NASA OBB Advanced Planning Team *Plan for Earth's Living Ocean: The Unseen World to Set NASA's Ocean Biology and Biogeochemistry Agenda* (NASA, in the press).